Grasping in the Dark: Compliant Grasping using Shadow Dexterous Hand and BioTac Tactile Sensor

Kanishka Ganguly, Behzad Sadrfaridpour, Krishna Bhavithavya Kidambi,
Cornelia Fermüller, Yiannis Aloimonos

***Abstract*— When it comes to grasping and manipulating objects, the human hand is the benchmark based on which we design and model grasping strategies and algorithms. The task of imitating human hand in robotic end-effectors, especially in scenarios where visual input is limited or absent, is an extremely challenging one. In this paper we present an adaptive, compliant grasping strategy using only tactile feedback. The proposed algorithm can grasp objects of varying shapes, sizes and weights without having a priori knowledge of the objects. The proof of concept algorithm presented here uses classical control formulations for closed-loop grasping. The algorithm has been experimentally validated using a Shadow Dexterous Hand equipped with BioTac tactile sensors. We demonstrate the success of our grasping policies on a variety of objects, such as bottles, boxes and balls.**

I. INTRODUCTION

Robotic agents, and their respective research fields, have generally proven useful in structured environments, crafted specifically for them to operate. Human environments contain scenes and objects designed for manipulation by anthropomorphic hands, not parallel grippers or suction cups. Stefanie Tellex, professor at Brown University, manages to succinctly summarize the current state of research in robotic grasping when she says that *most robots fail to grasp most objects most of the time* [1]. Having the ability to grasp robustly and repeatedly is the way by which robots can affect their environment, and is the first step to performing more complicated and involved tasks. For true anthropomorphic grasping, a combination of form factor of the hand as well as tactile sensing capabilities is crucial to replicate human-like range of motion and dexterity. We propose a novel pipeline and control algorithm implementation for robot grasping using the Shadow Dexterous Hand, equipped with the BioTac tactile sensors and augmented with external force sensitive resistors. Our pipeline allows for robust grasping of previously unseen objects of varied shapes, sizes, and weights without the need for visual feedback, due to reliance solely on tactile feedback. Humans are capable of this feat from an early age, and it is an important ability to have in scenarios with limited or occluded visual information. We demonstrate our pipeline on a variety of objects, including grasping transparent objects which traditional perception hardware have a difficult time detecting.

All authors are associated with the Perception and Robotics Group, University of Maryland, College Park, MD, 20740.
{kganguly, sadr, kidambi, fermulcm, jyaloimo}@umd.edu

II. PRIOR WORK

Research on robot grasping and manipulation focus predominantly on three main areas: (i) tactile sensing [2], [3], [4] (ii) perception [5], [6], [7] and (iii) learning [8], [9], [10] . Most of the progress in these areas have been in the perception and learning aspects, and developments in the field of tactile sensing for grasping has been generally sparse, due to lack of available hardware and the associated complexities [5]. The authors in [2] provide a wealth of information about tactile sensing in robot manipulation and [3], [4] provide a survey of recent literature on tactile sensing. They detail the the major tactile sensor types, modalities available, computational techniques and compare the usefulness of different tactile data, applications of tactile sensing for robotic grippers and provide insights into future directions. For a comprehensive review of the state of the art research, the readers are encouraged to go through the works in [3], [4] and the references included therein.

In [5], the authors demonstrate a data set of slow-motion actions (picking and placing) organized as manipulation taxonomies. In [6], an end-to-end action-conditioned grasping model is trained in a self-supervised manner that learns re-grasping from raw visuo-tactile data, where the robot receives tactile input intermittently. The work in [7] leverages the innovation in machine vision, optimization and motion generation to develop a low-cost glove-free teleoperation solution to grasping and manipulation. A reinforcement learning (RL) policy that can perform vision-based in hand manipulation is developed in [8]. The RL setup is trained in simulation and is transferred onto a five-fingered robot hand. A model-free deep RL which can be scaled up to learn variety of manipulation behaviours in the real world has been proposed in [9], using general purpose neural networks. A State-Only Imitation Learning (SOIL) is developed in [10], by training an inverse dynamics model to predict action between consecutive states. The research problems attempted using perception and learning has seen constrained progress due to the fact that vision does not provide any information regarding the contact forces, fails to reconstruct the scene due to occlusion or that the material properties of the object and the process of learning is time consuming, requires large amounts of data, and sometimes does not transfer into a real robot [11].

On the other hand tactile sensors provide robot hands with rich information about physical contact, as a result, autonomous robot hands can operate in unstructured environ-

Manuscript 2606 submitted to 2021 IEEE International Conference on Robotics and Automation (ICRA). Received October 31, 2020.

ments and manipulate unknown object [12], [13], [14], [15]. The work in [12], has presented an integration approach by extracting features from high-dimensional tactile images and infer relevant information to grasp quality. But the approach is restricted to flat, dome and edge-like shapes. A new tactile sensor "DIGIT" is presented in [13] that learns to manipulate small objects with a multi-fingered hand from raw, high-resolution tactile readings. The work by [15] uses a custom FingerVision [16] sensor to generate a set of tactile skills, such as stirring, in-hand rotation, and opening objects with specified force. In [17], the authors use the BioTac sensor as a way to stabilize objects during grasp using a grip force controller. The underlying assumption is that the shape of the object is known a priori and repeatability with different shapes and sizes still remains challenging.

III. APPROACH

Using a robotic hand equipped with tactile sensors and mounted on a robotic arm manipulator, our goal is to grasp an object and move it to another location. We define $\boldsymbol{q}_a \in \mathbb{R}^m$ and $\boldsymbol{q}_h \in \mathbb{R}^n$ as the vector of the joint positions of the robotic arm and robotic hand in the joint-space. Thus, the configuration of the robotic arm and hand can be represented by $\boldsymbol{q}_a$ and $\boldsymbol{q}_h$, respectively. For simplicity we define $\boldsymbol{q} = [\boldsymbol{q}_a^T,\ \boldsymbol{q}_h^T]^T \in \mathbb{R}^{m+n}$ as the representation of the robotic system. Moreover, the robotic hand configuration is consisted of the configurations of its fingers, i.e $\boldsymbol{q}_h = [\boldsymbol{q}_1^T, \boldsymbol{q}_2^T, \cdots \boldsymbol{q}_p^T, \boldsymbol{q}_r^T]^T$, where p is the number of the fingers and $\boldsymbol{q}_r$ is the joint angles not associated with any finger. The problem can be formulated as follows.

Given that an object is within the reach of the robotic system (with limited or minimal visual sensors), control the robotic system, i.e. $\boldsymbol{q}(t)$ trajectory, such that the object is manipulated to a desired location.

Our approach to solve this problem is to define different actions for the robot and plan the robot actions accordingly. Figure 1 shows the implementation of these actions. The details for controlling the robot to execute each of these actions are described in the rest of this section. Our proposed action planning approach is as follows.

- *Pre-Grasp* action: Move the robotic hand configuration, $\boldsymbol{q}_h$, to a pre-grasp configuration defined as $\boldsymbol{q}_{h,pre}$.
- *Pre-Grasp Object* action: Move the robotic arm configuration, $\boldsymbol{q}_a$, to a configuration near the object.
- *FSR Contact* action: Control the finger i configuration, $\boldsymbol{q}_i$, such that its Proximal phalanges (the nearest phalanges to the palm) reaches the object.
- *Switch Joints* action: Control the finger i configuration, $\boldsymbol{q}_i$, such that its Distal phalanges (the fingertip) reaches the object.
- *Raise Arm* action: Move the robotic arm configuration, $\boldsymbol{q}_a$, upwards while controlling the robotic hand configuration $\boldsymbol{q}_h$ to prevent object slippage.

The setup that we use to implement our pipeline includes multiple different robotic and sensing hardware, primarily the UR-10 manipulator and the Shadow Dexterous Hand, equipped with SynTouch BioTac tactile sensors [18]. Our approach utilizes a multi-level controller architecture, where we deploy different strategies for controlling the UR-10 arm and the Shadow Hand [19] with feedback between controllers. The underlying control inputs come from various tactile sensors and the joint angles of the Shadow Hand.

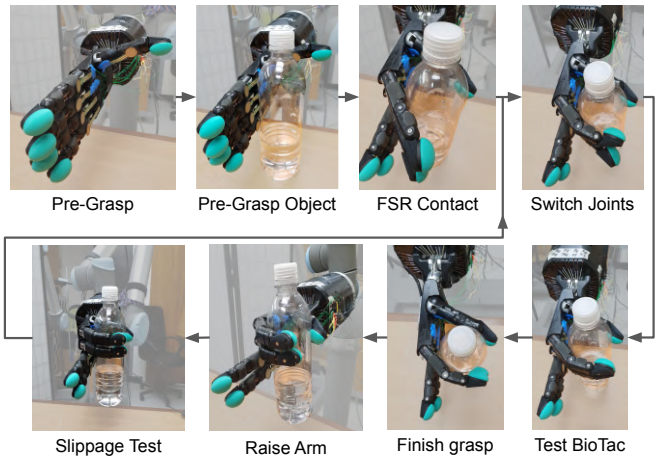

Fig. 1: Grasp Pipeline Demonstration

A. Kinematic Structure of the Shadow Dexterous Hand

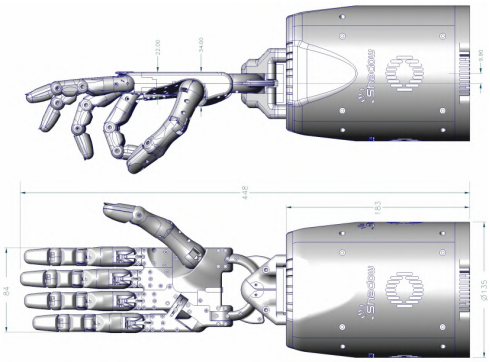

Fig. 2: Shadow Hand Structure

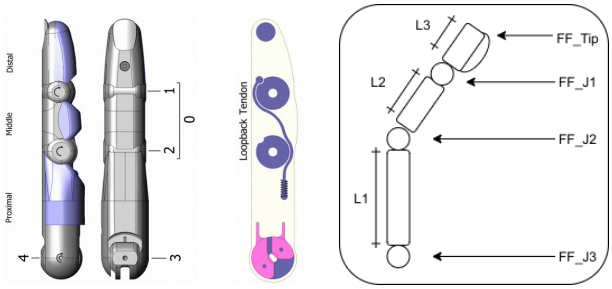

(a) Finger (b) Thumb (c) Joints

Fig. 3: Shadow Hand (a) finger and (b) thumb, and (c) their corresponding finger joint positions diagrams

It is important to understand the basic structure of each finger of the Shadow Dexterous Hand since that determines how the controller behaves when grasping different objects.

We will also provide a brief understanding of the characteristics of the SynTouch BioTac sensors and how they operate. The Shadow Dexterous Hand is a biomimetic robotic hand that provides a physical range of motion and kinematic structure very similar to that of the human hand. It does this using a combination of accurate joint positions and link lengths as well as replicating the form factor using a thread-and-pulley system of actuation. The three fingers on the Shadow Hand, namely the first, middle and ring fingers, have a similar kinematic structure and is described by Fig. 3a and contain four movable joints. The thumb is different from the others in that it has a greater range of motion and thus has 5 degrees of freedom. This is described in Fig. 3b. The little finger, while similar to the first three fingers kinematically, has an extra joint in the palm which allows it to oppose the thumb in an effort to be anatomically correct. Figure 3c shows a simplified diagram of one finger and the joints specification it follows. Each finger has three links, also called phalanges, with one joint in between. From top of the finger to the base, these are called the distal, middle and proximal phalanges respectively. Each joint is prefixed by the finger it belongs to, i.e. first finger has prefix `FF_`, middle finger has prefix `MF_` and so on.

The fingers can be controlled by sending joint position values. The joint J_3 has two controllable ranges of motion, along the *sagittal* and *transverse* axes. This joint also has a minimum and maximum range of $0°$ to $90°$ respectively. The joints J_1 and J_2 are different in that, similar to the human hand, they are coupled internally at a kinematic level and do not move independently. They individually have a range of motion between $0°$ to $90°$, but are underactuated. This means that the angle of the middle joint, i.e. J_2 is always greater than or equal to the angle of the distal joint, i.e. J_1 which allows the middle phalanx to bend while the distal phalanx remains straight. In software, they are controlled jointly using the J_0 identifier. We postulate that

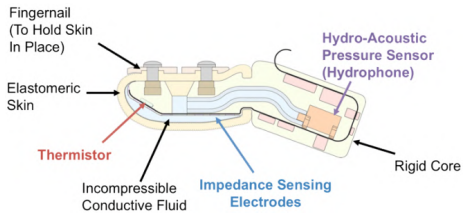

Fig. 4: BioTac Sensor Cross-Section

tactile sensors, as they currently exist, lie on a spectrum spanning from accuracy on one end to form factor on the other. Artificial tactile sensors can either have high accuracy while sacrificing anthropomorphic form factors or can be designed similar to human fingers or skin, while having a relatively poor accuracy at tactile sensing. Depending on the use case and tasks that the end-effector these sensors are attached to need to perform, one might prefer one style over the other. In our experiments, considering the biomimetic design of the Shadow Dexterous Hand, we have used the BioTac tactile sensors from SynTouch. These sensors are shaped very similar to the human finger tip, and behave mechanically similar to that as well. The BioTac sensors employ an interesting design principle, it consists of an elastomeric "skin" that covers a set of sensors. The skin serves the purpose of containing a conductive liquid that provides the anthropomorphic sensing capabilities, as well as allows for deformation due to shear when in contact with surfaces. The conductive liquid is the main component that transmits tactile information from the surface in contact with the skin to the sensors underneath.

Using a combination of impedance sensing electrodes, hydro-acoustic pressure sensors and thermistors, the BioTac sensor is capable of sensing three of the most important sensory inputs that one needs for grasping, namely deformation and motion of stimuli across the skin, the pressure being applied on the finger and temperature flux across the surface. The internal cross-section of the BioTac is shown in Fig. 4.

(a) FSRs (b) Connections (c) Contact Regions

Fig. 5: FSRs and Their Connection to Arduino Nano, an,d Regions of Contact When Grasping

The human hand can grasp objects of various shapes, sizes and masses without having seen them previously. This ability to grasp previously unseen objects in the absence of visual cues is possible only due to the presence of tactile sensing over a large surface area, through the skin. In Fig. 5c, the highlighted parts show the primary regions of contact when grasping is performed. These regions make first contact with the object being grasped and apply the most amount of force, due to the large surface area. To mimic similar tactile characteristics on the Shadow Dexterous Hand, we equip it with additional sensors at the base of each finger and the thumb.

We utilize force sensitive resistors for this, which are flexible pads that change resistance when pressure is applied to the sensitive area. These sensors are positioned as shown in Fig. 5a and wired up to an Arduino microcontroller, as shown in Fig. 5b. The force sensitive resistors work on the principle of a voltage divider circuit and have a voltage drop inversely proportional to the resistance of the FSR. This can be computed using the formula $V_{\text{out}} = V_{\text{cc}} \times \frac{\Omega_{\text{resistor}}}{(\Omega_{\text{resistor}} + \Omega_{\text{fsr}})}$. We calibrate our sensors using a ground-truth force measurement unit, for 0N to 50N of force. This is sufficient to measure contact forces between the fingers and an object during grasping.

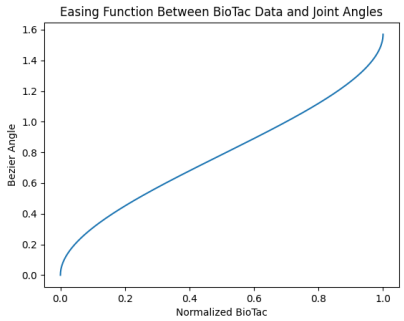

Fig. 6: Beziér Easing Function

B. Grasp Controller

Since we attempt to grasp objects without any visual input, our grasp controller makes the assumption that the Shadow Hand is positioned appropriately near the object, within the bounds of the trajectory of the fingers and thumb. This stage is termed the pre-grasp pose and we use a repeatable algorithm to start our controller from this stage. At the pre-grasp stage, the fingers are fully extended and the thumb is bent at the base to a 70° angle, which is optimal for grasping most objects due to having the maximum volume coverage by the trajectories of the finger tips. The controller begins by performing a tare operation using 50 readings of each BioTac sensor and computing the mean. Successive readings are min-max normalized, within an adjustable threshold of ± 200 of this mean, to ensure that each sensor's biases are taken into account, as well as to provide a standardized input to the control loop.

Once the initialization process is complete and baseline readings have been established, the hand controller begins actuating the J_3 joints of all the fingers and J_4 of the thumb. This is done by sending the appropriate joint control commands published as a ROS message. The current joint values are obtained from the Shadow Hand, checked against the maximum joint limits of each finger (90° for J_3), and increased by a small angle θ_Δ. The J_3 and J_4 joints of the fingers and thumb respectively are moved until it registers a contact with the object, as measured by the FSR readings. This establishes an initial reference point for the Hand to begin refining the grasp, and the controller switches to a different control policy at this stage.

At this stage, since the base of each finger and thumb have made initial contact with the object, the control policy switches to the higher joints so that the fingers can begin to "wrap around" the object. We now activate the coupled J_0 joints of the fingers and the J_1 joint on the thumb. In this stage, the θ_Δ is computed using a heuristic control policy. Since our BioTac data is normalized between 0 and 1, we perform an inverse mapping between the normalized sensor data and a previously initialized minimum and maximum joint angle value θ_{min} and θ_{max} respectively. This means that when there is little or no contact between the fingers and the object, the controller sends out larger joint angle targets causing the fingers to move larger distances. Once contact is made, the controller moves the fingers at progressively smaller increments, thus allowing for a more stable and refined grasp.

We use a Beziér curve to generate an easing function that maps our normalized BioTac sensor data to a normalized angle (in radians), between the joint limits of the respective joint. This mapping then gets converted into a usable control output between θ_{min} and θ_{max}. The Beziér curve is generated by the parametric formula $\theta_\beta = S^2_{\text{BioTac}} \times (\kappa_1 - (\kappa_2 \times S_{\text{BioTac}}))$ where κ_1 and κ_2 are the Beziér control points, S_{BioTac} is the BioTac reading and θ_β is the mapped Beziér curve output. We then compute $\theta_\Delta = B_1 + \frac{(\theta_\beta - A_1)\times(B_2 - B_1)}{A_2 - A_1}$ where $[A_2, A_1]$ and $[B_2, B_1]$ range between $[0, 1]$ and $[\theta_{\text{min}}, \theta_{\text{max}}]$ respectively.

We set a termination threshold $\tau_{\text{termination}}$ on the BioTac sensor values such that the Hand controller stops executing as soon as a minimal level of contact is detected. Once all the fingers and the thumb have reached the preliminary grasp state, we exit the control loop.

Algorithm 1 Implementation of the initial grasp controller

procedure RESET SEQUENCE
  repeat
    Move Hand to pre-grasp pose
  until `grasp_is_possible`
end procedure
procedure INITIALIZE BASELINES
  for finger $\in$ all fingers **do**
    $\text{baseline}_{\text{finger}} \leftarrow \frac{\sum_{n=1}^{50} P_{dc}}{n}$ ▷ Set baselines
  end for
end procedure
repeat
  Fetch current J_3 state
  $J_3 \leftarrow J_3 + \theta_\Delta$
  Actuate J_3 ▷ Move J_3 towards object
until FSR registers contact ▷ $L1$ touches object
Switch Control Policy
$\kappa_1 \leftarrow 3.0$, $\kappa_2 \leftarrow 2.0$
repeat
  procedure COMPUTE CONTROL OUTPUT
    Get S_{BioTac}
    $\theta_\beta = S^2_{\text{BioTac}} \times (\kappa_1 - (\kappa_2 \times S_{\text{BioTac}}))$
    $\theta_\Delta = B_1 + \frac{(\theta_\beta - A_1)\times(B_2 - B_1)}{A_2 - A_1}$
  end procedure
  while $J_1 + J_2 \leq 180^\circ$ **do**
    Fetch current J_2 state
    Fetch current J_1 state
    if J_2 not obstructed **then**
      $J_2 \leftarrow J_2 + \theta_\Delta$
      Actuate J_2 ▷ Move J_2 towards to object
    else
      $J_1 \leftarrow J_1 + \theta_\Delta$
      Actuate J_1 ▷ Move J_1 towards to object
    end if
  end while
until $P_{dc} \geq \tau_{\text{termination}}$ ▷ Fingertip touches object

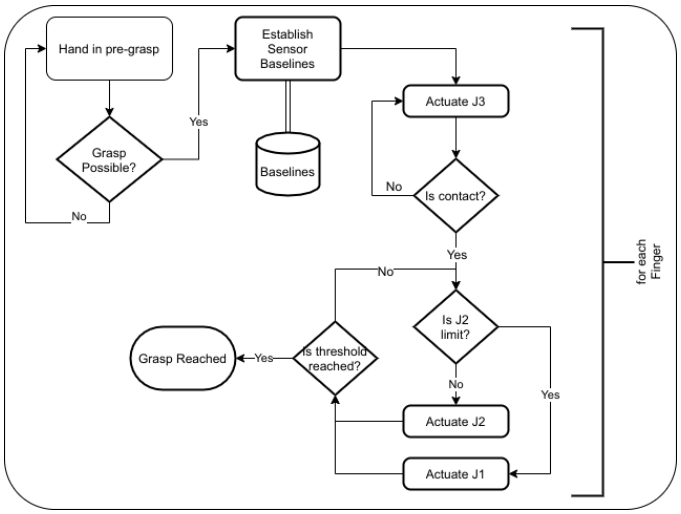

Fig. 7: Grasp Controller Architecture

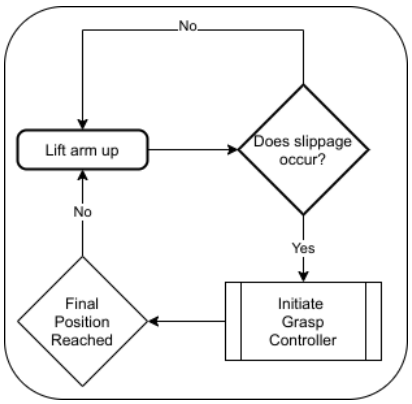

Fig. 8: UR-10 Controller Architecture

Algorithm 2 Implementation of picking with slip detection

```
procedure SLIPPAGE DETECTOR
    while Hand has not reached its goal do
        repeat
            Actuate J_1          ▷ Push J_1 towards to object
        until P_dc ≥ τ_non_slip      ▷ L_3 tightens the object
        repeat
            Move UR-10 upwards
        until slip detected
    end while
end procedure
```

C. UR-10 Controller Architecture

Once we have established an initial grasp on the object, we switch our controller to command the UR-10 manipulator. Since we are attempting a pick and place operation, the success or failure of the pipeline depends on the ability to grasp and lift the object consistently and robustly for a certain period of time. Since the UR-10 and Shadow Hand are two separate kinematic chains, their respective robot models are attached at a fixed wrist joint. This allows us to apply our inverse kinematic operations to the wrist of the UR-10 in order to move the Shadow Hand.

We raise the UR-10's end-effector by a small amount upwards, thus removing the grasped object from the surface on which it is placed. This, coupled with the fact that the initial grasp is intentionally loose, causes the object to start sliding downwards due to its weight. Simultaneously, while the arm is being raised, we execute our slippage detection subroutine to obtain data from the BioTac sensors and check if the object is slipping between the fingers. If a slip is detected, we immediately stop execution on the arm controller and switch to the Grasp Controller. However, this is done with dynamically updated threshold parameters, based on the measured value of the slip. A greater slip coefficient implies that a faster and tighter grasp actuation is required and vice versa. We explain our slip detection algorithm in the subsequent section. Once the grasp adjustment process is complete, we resume our arm controller and continue this controller switching pipeline until the UR-10 reaches its desired final pose.

D. Slippage Detection

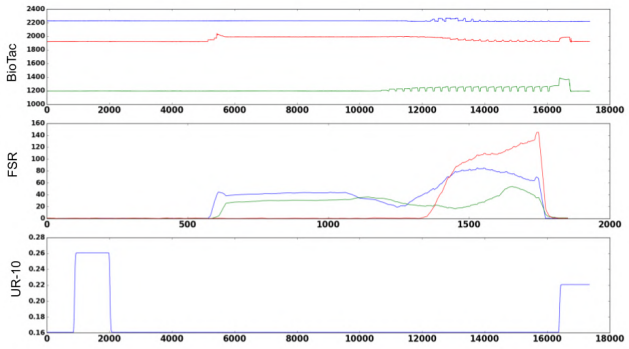

Fig. 9: Plot of Sensor Data During Slip

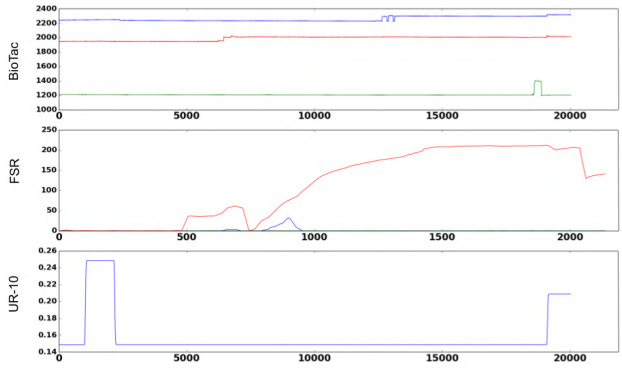

Fig. 10: Plot of Sensor Data Without Slip

One of the crucial aspects of our proposed grasping pipeline is the ability to detect, and react to objects slipping between the fingers during grasp and move. This reactive nature of our controller allows for precise force applications on the object, without knowing the masses, sizes or shapes of the objects a-priori. At the same time, we are able to adjust our grasp to hold objects with dynamically changing masses,

such as water being poured into a bottle.

We employ sensor readings from both the BioTac as well as the FSRs. Figs. 9 and 10 show two sets of plots of sensors readings captured during grasping a bottle, with and without slip respectively. Figs. 9 and 10 graphs represent the BioTac, FSR readings and the position of the UR-10. For visual clarity, we plot data for only the first and middle fingers and the thumb. The difference in readings during slip vs. without slip is quite evident, with several micro-vibrations in the BioTac data while the object slowly falls off the Hand. This is due to the frictional properties of the BioTac skin, as well as the weight of the object. Similar vibrations are absent when the object does not slip, and the readings maintain a mostly stable baseline.

Our slip detection algorithm works by measuring and tracking the change in gradient at time t of the readings with respect to the previous gradient at time $t-1$. We use linear regression [20] on a circular buffer to obtain a constantly updating slope, and perform the comparison at specific intervals. Since both BioTac and FSR sensors are time synchronized through ROS, we can perform a concurrent check of the changes and if both sets of readings concur, we detect a slip event. Consequently, by measuring the relative change in gradient, we are able to judge how fast the object is slipping, and provide larger or smaller control commands as necessary. The gradient is computed as $\frac{\sum_{i=1}^{n}(y_i-\overline{Y})\times(x_i-\overline{X})}{\sum_{i=i}^{n}(x_i-\overline{X})^2}$.

IV. EXPERIMENTS AND RESULTS

A. Experiment Setup

Our hardware setup consists of a UR-10 manipulator, to which the Shadow Dexterous Hand is attached. The FSR runs on an Arduino microcontroller connected to an ODroid-XU4 single-board computer. The main controller pipeline is written in C++, in an effort to be time-sensitive and performant. We also introduce the `shadowlib` library, a software toolkit that contains several utility functions for controlling the Shadow Hand. The code is hosted on Github and available on request.

B. Networking and Pipeline

The grasp controller works by simultaneously obtaining tactile feedback from the FSRs and the BioTac and using that to output appropriate control commands to both the UR-10 and the Shadow Hand. We use the Robot Operating System (ROS) as the communication paradigm, which allows for easy message passing between the various components of our pipeline. The Shadow Hand communicates with the main control PC via the EtherCAT protocol and uses the provided ROS drivers. The Hand receives a target joint angle to reach, and an onboard inner loop position controller then executes the corresponding motor until the target is reached. The UR-10 interfaces using the dedicated control box that processes commands sent via the ROS driver, and uses a proprietary URScript format for message passing. The FSRs are connected to an Arduino, that uses the `pyserial` library to stream the data to a python script running on an ODroid-XU4 single board computer which then converts it to a set of appropriate ROS messages and publishes them for subscription on the main controller PC.

TABLE I: Summary of Results

Objects	Type	Pass	Fail	Succcess (%)
Cup	Cylinder	4	1	80
Glass	Cylinder	4	1	80
Football	Sphere	3	2	60
Softball	Sphere	4	1	80
Sugar	Cuboid	2	3	40
Electronic Box	Cuboid	4	1	80

C. Results

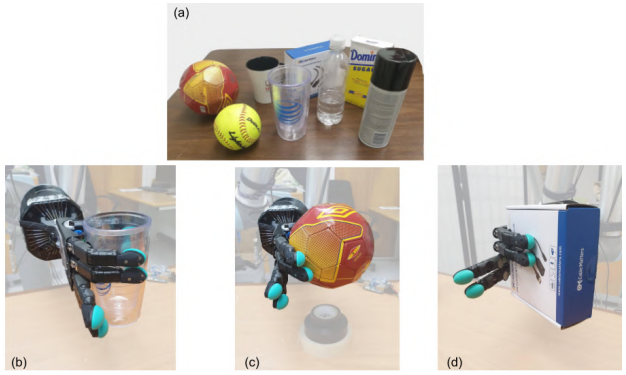

Fig. 11: Dataset and Results

We demonstrate our algorithm on a set of objects with varied shapes and sizes. Fig. 11a shows the dataset used, and three successful grasps of three types of objects, namely cylindrical, spherical and cuboidal in Fig. 11b, 11c, and 11d respectively. We are able to grasp a glass (13b), a ball (13c) and a box (13d) without any human intervention and without prior knowledge of their shapes, sizes or weights. The only assumption was that the objects were placed in reach of the Hand. The criteria for successful grasp were the ability to not only grasp the object entirely, but also to lift it and hold it in place for 10 seconds. Table I summarizes our results for various objects in our dataset. The accompanying video submission shows a detailed view of the grasping process, with cases for slip and without, as well as results for the other objects.

V. CONCLUSIONS

In this proposed work, we develop a simple closed-loop formulation to grasp and manipulate and object with just tactile feedback using Shadow Dexterous Hand with BioTac Tactile sensors. They achieve human like form factor without compromising on the accuracy. The algorithm presented here is a proof-of concept and uses classical control formulations for closed-loop compliant grasping. The main contributions of the paper are summarised as: (1) Developed a proof-of concept closed-loop algorithm for compliant grasping with only tactile feedback and without prior information about the objects, (2) The proposed algorithm can grasp objects of different sizes, shapes and configurations, (3) The proposed method has been experimentally tested on a Shadow Dexterous Hand with BioTac tactile sensors. In future work, we plan to explore more advanced control formulations, include vision as a method to automate the pre-grasp pipeline and validate our results on a diverse dataset.

Manuscript 2606 submitted to 2021 IEEE International Conference on Robotics and Automation (ICRA). Received October 31, 2020.

REFERENCES

[1] W. Knight, "Robot, get the fork out of my sink," Apr 2020. [Online]. Available: https://www.technologyreview.com/2016/10/18/69877/robot-get-the-fork-out-of-my-sink/

[2] H. Yousef, M. Boukallel, and K. Althoefer, "Tactile sensing for dexterous in-hand manipulation in robotics—a review," *Sensors and Actuators A: physical*, vol. 167, no. 2, pp. 171–187, 2011.

[3] Z. Kappassov, J.-A. Corrales, and V. Perdereau, "Tactile sensing in dexterous robot hands," *Robotics and Autonomous Systems*, vol. 74, pp. 195–220, 2015.

[4] A. Yamaguchi and C. G. Atkeson, "Recent progress in tactile sensing and sensors for robotic manipulation: can we turn tactile sensing into vision?" *Advanced Robotics*, vol. 33, no. 14, pp. 661–673, 2019.

[5] Y. C. Nakamura, D. M. Troniak, A. Rodriguez, M. T. Mason, and N. S. Pollard, "The complexities of grasping in the wild," in *2017 IEEE-RAS 17th International Conference on Humanoid Robotics (Humanoids)*. IEEE, 2017, pp. 233–240.

[6] R. Calandra, A. Owens, D. Jayaraman, J. Lin, W. Yuan, J. Malik, E. H. Adelson, and S. Levine, "More than a feeling: Learning to grasp and regrasp using vision and touch," *IEEE Robotics and Automation Letters*, vol. 3, no. 4, pp. 3300–3307, 2018.

[7] A. Handa, K. Van Wyk, W. Yang, J. Liang, Y.-W. Chao, Q. Wan, S. Birchfield, N. Ratliff, and D. Fox, "Dexpilot: Vision-based teleoperation of dexterous robotic hand-arm system," in *2020 IEEE International Conference on Robotics and Automation (ICRA)*. IEEE, 2020, pp. 9164–9170.

[8] O. M. Andrychowicz, B. Baker, M. Chociej, R. Jozefowicz, B. McGrew, J. Pachocki, A. Petron, M. Plappert, G. Powell, A. Ray *et al.*, "Learning dexterous in-hand manipulation," *The International Journal of Robotics Research*, vol. 39, no. 1, pp. 3–20, 2020.

[9] H. Zhu, A. Gupta, A. Rajeswaran, S. Levine, and V. Kumar, "Dexterous manipulation with deep reinforcement learning: Efficient, general, and low-cost," in *2019 International Conference on Robotics and Automation (ICRA)*. IEEE, 2019, pp. 3651–3657.

[10] I. Radosavovic, X. Wang, L. Pinto, and J. Malik, "State-only imitation learning for dexterous manipulation," *arXiv preprint arXiv:2004.04650*, 2020.

[11] Y. Liu, Z. Li, H. Liu, and Z. Kan, "Skill transfer learning for autonomous robots and human-robot cooperation: A survey," *Robotics and Autonomous Systems*, p. 103515, 2020.

[12] N. Pestell, L. Cramphorn, F. Papadopoulos, and N. F. Lepora, "A sense of touch for the shadow modular grasper," *IEEE Robotics and Automation Letters*, vol. 4, no. 2, pp. 2220–2226, 2019.

[13] M. Lambeta, P.-W. Chou, S. Tian, B. Yang, B. Maloon, V. R. Most, D. Stroud, R. Santos, A. Byagowi, G. Kammerer *et al.*, "Digit: A novel design for a low-cost compact high-resolution tactile sensor with application to in-hand manipulation," *IEEE Robotics and Automation Letters*, vol. 5, no. 3, pp. 3838–3845, 2020.

[14] F. R. Hogan, M. Bauza, O. Canal, E. Donlon, and A. Rodriguez, "Tactile regrasp: Grasp adjustments via simulated tactile transformations," in *2018 IEEE/RSJ International Conference on Intelligent Robots and Systems (IROS)*. IEEE, 2018, pp. 2963–2970.

[15] B. Belousov, A. Sadybakasov, B. Wibranek, F. Veiga, O. Tessmann, and J. Peters, "Building a library of tactile skills based on fingervision," 2019, pp. 717–722.

[16] A. Yamaguchi, "Fingervision," http://akihikoy.net/p/fv.html, 2017.

[17] F. Veiga, B. Edin, and J. Peters, "Grip stabilization through independent finger tactile feedback control," *Sensors (Basel, Switzerland)*, vol. 20, no. 6, p. 1748, Mar 2020. [Online]. Available: https://pubmed.ncbi.nlm.nih.gov/32245193

[18] "https://www.syntouchinc.com/en/sensor-technology/." [Online]. Available: https://www.syntouchinc.com/en/sensor-technology/

[19] P. Tuffield and H. Elias, "The shadow robot mimics human actions," *Industrial Robot: An International Journal*, 2003.

[20] J. M. Stanton, "Galton, pearson, and the peas: A brief history of linear regression for statistics instructors," *Journal of Statistics Education*, vol. 9, no. 3, p. null, 2001. [Online]. Available: https://doi.org/10.1080/10691898.2001.11910537